Applied Surface Science 258 (2012) 5001–5004

Contents lists available at SciVerse ScienceDirect

Applied Surface Science

journal homepage: www.elsevier.com/locate/apsusc

Thermal reliability of thin SiGe epilayers

Ming-Jhang Wu[a,1], Hua-Chiang Wen[b,*,1], Tun-Yuan Chiang[c], Chien-Huang Tsai[d], Wen-Kuang Hsu[b], Chang-Pin Chou[a]

[a] Department of Mechanical Engineering, National Chiao Tung University, Hsinchu 300, Taiwan, ROC
[b] Department of Materials Science and Engineering, National Tsing Hua University, Hsinchu, 30013, Taiwan, ROC
[c] Department of Mechanical Engineering, Chin-Yi University of Technology, Taichung 411, Taiwan, ROC
[d] Department of Automation Engineering, Nan Kai University of Technology, Nantou 54243, Taiwan, ROC

ARTICLE INFO

Article history:
Received 30 September 2011
Received in revised form
24 November 2011
Accepted 21 December 2011
Available online 28 December 2011

Keywords:
SiGe
Ultrahigh-vacuum chemical vapor deposition
AFM
Nanoscratch

ABSTRACT

The SiGe heterostructures can play a role that drastically enhances the carrier mobility of SiGe heterodevices, such as strained Si metal oxide semiconductor field effect transistors. However, it is difficult to access the both issues, that is, the propagation of the dislocation and thermal reliability of annealed SiGe films. In this study, we used ultrahigh-vacuum chemical vapor deposition to grow $Si_{0.8}Ge_{0.2}$ films (ca. 200 nm thick for heteroepitaxy) epitaxially on bulk Si. The samples were subsequently furnace-crystallized at temperatures of 800, 900, and 1000 °C. We used nanoscratch techniques to determine the frictional characteristics of the SiGe epilayers under various ramping loads and employed atomic force microscopy to examine their morphologies after scratching. From our investigation of the pile-up phenomena, we observed significant cracking dominating on both sides of the scratches on the films. The SiGe epilayers films that had undergone annealing treatment possessed lower coefficients of friction, suggesting higher shear resistances.

1. Introduction

SiGe is an outstanding semiconductor material because of its attractive characteristics [1–3]. High Ge-content strained SiGe-on-Si is a useful channel material in high-mobility SiGe-channel p-type metal oxide semiconductor field-effect transistors [4–7]. The performance of Si very-large-scale integration (VLSI) chips is improved considerably through the application of SiGe heterostructures; as a result, much effort is being exerted in this field, ranging from material growth to device design. SiGe heterostructures will undoubtedly be implemented in some important VLSI systems. Nevertheless, the growth of SiGe on bulk Si remains a challenge because of the 4% lattice mismatch between Si and Ge and because of the onset of misfit dislocation formation above the critical thickness [8,9]. As a result, strain relaxation-induced crystal defects, such as misfit dislocations and threading dislocations from interfaces [10,11], can occur, thereby worsening the mechanical characteristics of the SiGe epilayers. The presence of high-quality SiGe is an important issue affecting the reliability of device applications; crystal defects are to be avoided [12,13].

Although SiGe grown epitaxially on bulk Si typically has a different lattice parameter from that of the substrate, such films undergo elastic deformation, according to Poisson's ratio, to accommodate the lattice mismatch on both the film and the substrate. Because of the strain in the film, the elastic energy increases linearly upon increasing the film thickness. The critical thickness [14] is the film thickness over which the introduction of misfit dislocations into the film becomes energetically favorable. More unstable structures are formed when the films are thicker; indeed, when the film thickness reached 500 nm, large numbers of dislocations occur even when the treatment temperature is below the deposition temperature. In a previous study [15], we evaluated the nanotribological properties of 500-nm-thick SiGe films after annealing treatment. In that study, the SiGe epilayers were in a metastable state because their thickness was greater than the critical thickness; indeed, during low-temperature thermal treatment, strain relaxation occurred when the thickness was greater than 300 nm. In general, SiGe epilayers exhibit poor interfacial adhesion and are susceptible to debonding, resulting in low reliability during their manufacture. Indentation systems are suitable tools for measuring the mechanical properties—including adhesion—of these films to their substrates [16–21]. Several factors, including the degrees of sliding and abrasive wear, the sliding load, the sliding speed, and the surface roughness, can all impact the wear values of thin SiGe epilayers.

In this study, we employed ultrahigh-vacuum chemical vapor deposition (UHV/CVD) to deposit SiGe epilayers, which we then subjected to annealing. We used atomic force microscopy (AFM) and nanoscratch techniques to characterize the surface

* Corresponding author. Tel.: +886 3 5712121; fax: +886 03 5733409.
E-mail address: a091316104@gmail.com (H.-C. Wen).
[1] The first and second author contributed equally to this work.

0169-4332/$ – see front matter © 2011 Elsevier B.V. All rights reserved.
doi:10.1016/j.apsusc.2011.12.101

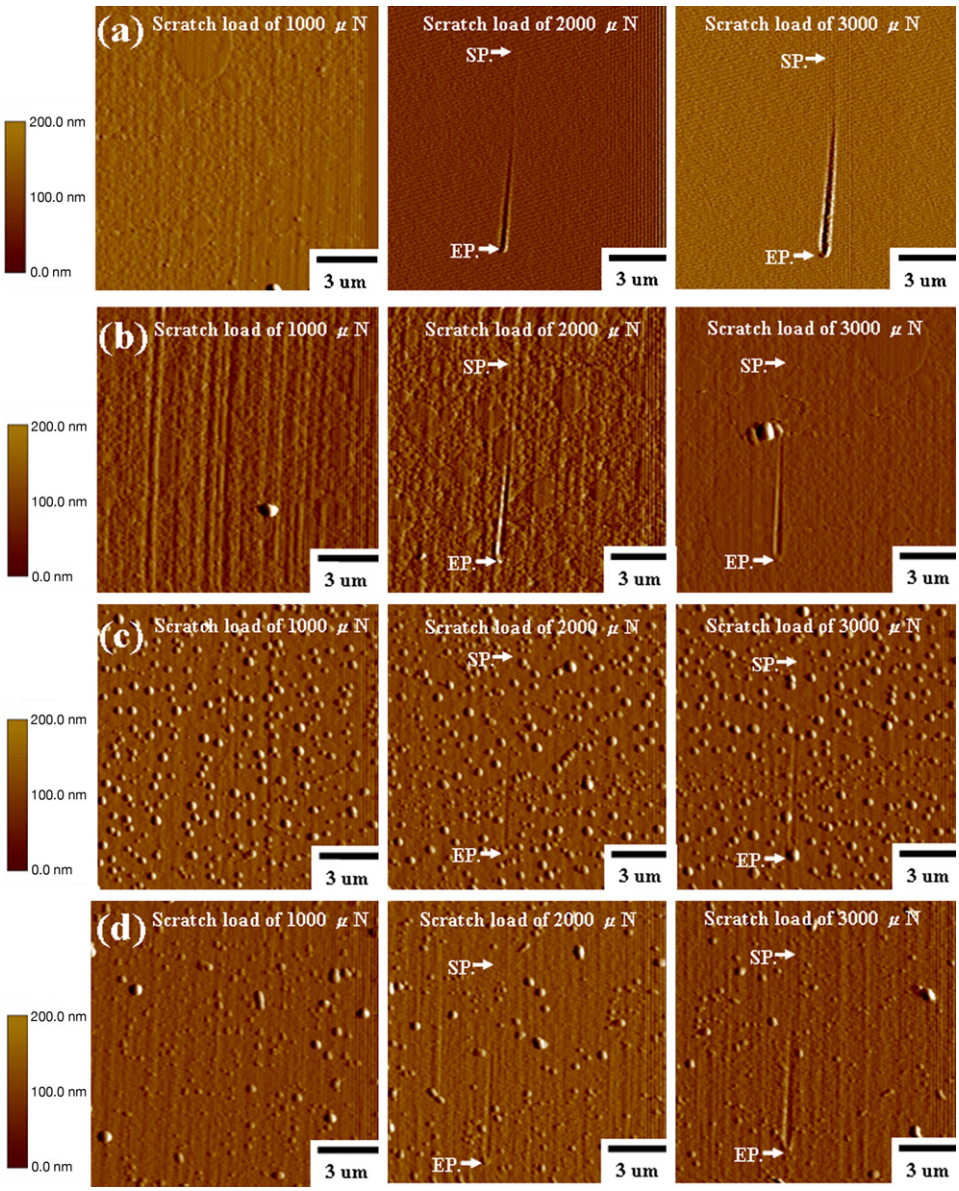

Fig. 1. 2-D AFM images of scratch tracks on the (a) as-deposited SiGe thin film and (b–d) SiGe thin films that had been subjected to thermal treatment at (b) 800, (c) 900, and (d) 1000 °C *ex situ* in a furnace under N_2 for 30 min. All of these samples had been subjected to ramping loads of 1000, 2000, and 3000 μN to obtain the surface profiles.

morphologies and tribological properties. We found that studying the nanotribological behavior is a convenient tool for determining the adhesive or cohesive strength of 200-nm-thick SiGe epilayers.

2. Experimental procedure

Samples were prepared beginning with a standard Radio Corporation of American (RCA) clean and washing for 15 s in a HF:H_2O (1:50) bath; the p-type Si(1 0 0) wafers were then introduced simultaneously into the load-lock chamber of the UHV/CVD system. The deposition process involved three steps: (i) a 3-nm-thick Si buffer layer was deposited on the Si substrate at 500 °C for 30 min from pure SiH_4 (in 85 sccm) gas at a rate of deposition of 0.1 nm/min; (ii) a 200-nm-thick $Si_{0.8}Ge_{0.2}$ epilayer was deposited at 500 °C for 70 min from a mixture of pure SiH_4 (in 85 sccm) and GeH_4 (in 15 sccm) at a rate of deposition of 2.8 nm/min under a vacuum of 10^{-7} mbar; (iii) the SiGe epilayers were subjected to thermal treatment (800, 900, or 1000 °C) *ex situ* in a furnace under N_2 gas for 30 min. The details of the UHV/CVD growth process of such samples have been reported previously [21].

To identify the nanotribological properties of the samples, an atomic force microscope (Digital Instruments Nanoscope III) and a nanoindentation measurement system (Hysitron) were used to perform the nanoscratch tests, in which a ramping load (1000, 2000 and 3000 μN) was applied at a constant scan speed of 2 $\mu m\,s^{-1}$ to the annealed samples. Surface profiles before and after scratching were obtained through tip-scanning at a normal load of 0.02 mN. After scratching, the wear tracks were imaged by AFM.

3. Results and discussion

The nanoscratch technique has been employed widely to investigate the nanotribological properties of thin films. Such tests have revealed that film's hardness can be enhanced through strain relaxation after thermodynamic treatment or that films that are more susceptible to plastic deformation are influenced by dislocation-induced additional strain. We used AFM to analyze all of our

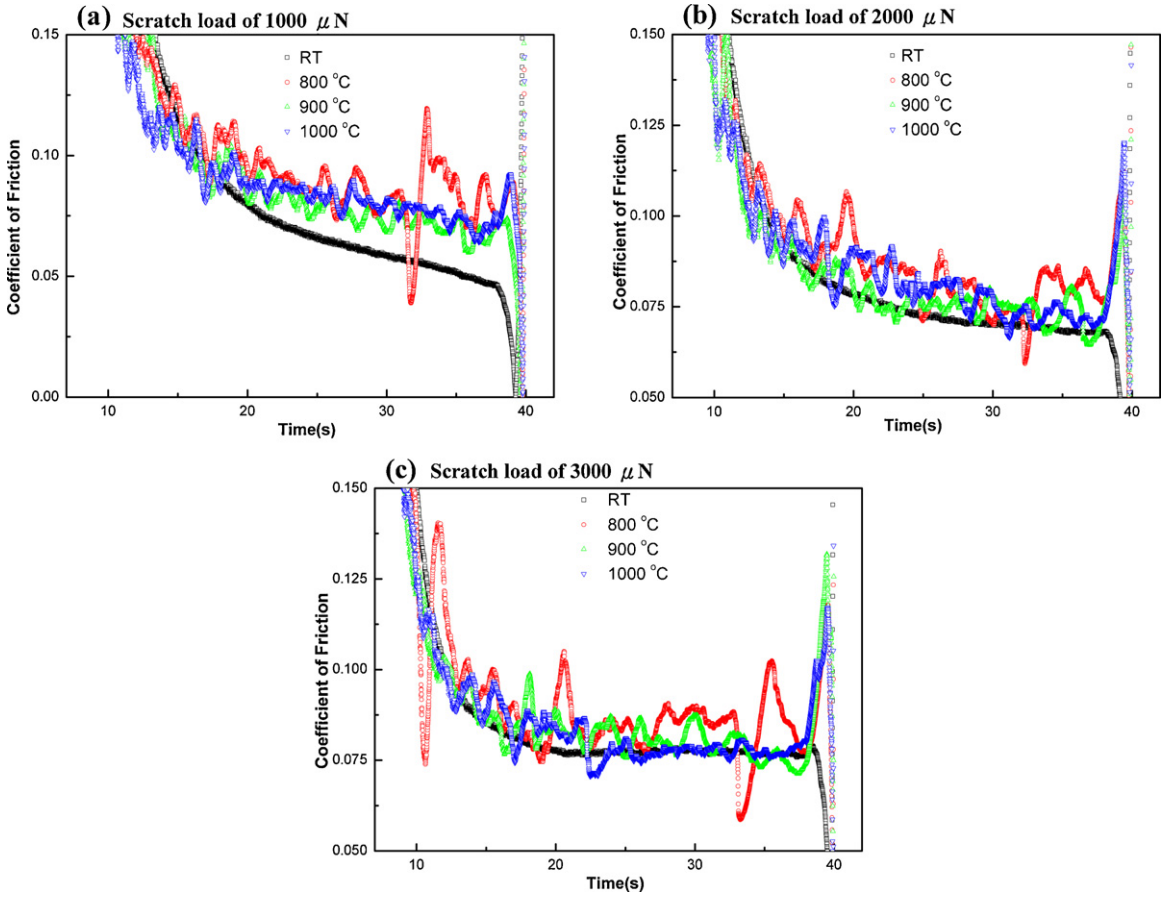

Fig. 2. Typical profiles of the COF plotted with respect to the scratch duration. The samples had been subjected to ramping loads of (a) 1000, (b) 2000, and (c) 3000 μN to obtain the surface profiles.

samples under ramping loads of 1000, 2000, and 3000 μN. Fig. 1(a) displays images of SiGe epilayers grown directly on the Si(0 0 1) substrate at room temperature (RT). From the ramping load scratch tests (see the image in the inset), we found that the film failed immediately upon increasing the applied load. Fig. 1(b)–(d) present images of the SiGe epilayers annealed at temperatures of 800, 900, and 1000 °C, respectively. Nanoscratch testing caused material pile-up to occur at the end and sides of each scratch track. The scratching of the samples at a load of 1000 μN was low relative to those at 2000 and 3000 μN; indeed, scratch tracks were not evident [Fig. 1(a)–(d)], presumably because of elastic reaction resulting from elastic deformation between the groove and film. The start point (SP) and end point (EP) of the tip is marked for each sample subjected to ramping loads of 2000 and 3000 μN. From a detailed investigation of SiGe epilayers, He et al. [22,23] found that 200- and 500-nm-thick $Si_{0.8}Ge_{0.2}$ epilayers exhibited comparable behavior. Fig. 1 reveals, however, that the transition from purely elastic to elastoplastic contact occurred only upon initially applying a ramped force of 2000 μN; total plastic contact occurred only slightly. In this scenario, we suggest that a slightly machined surface without cracks might be induced from the ductile-regime machining part (elastoplastic deformation) of the scratch track. Lin et al. [24] also reported the observation of elastoplastic contact. AFM images clearly revealed that the degree of pile-up and the depth of the groove along the z-direction both increased upon increasing the sliding distance.

Fig. 2 presents typical profiles of the coefficient of friction (COF) plotted with respect to the scratch duration, obtained as the ratio of the *in situ*-measured tangential force to the applied ramping load (1000, 2000, or 3000 μN), and the degree of annealing. We observe stable profiles of the COF for each ramping load of the SiGe epilayers at RT. Notably, the μ profiles of the SiGe epilayers oscillated relatively irregularly, due to strong bonds and cohesive failure from the period of transition of the SiGe epilayers annealed at 800 °C; quite regular oscillating profiles, caused by weak bonds of cohesive failure from the period of transition, were evident for the sample annealed at 900 °C; nanoscratch-induced deformation occurred on the SiGe epilayers annealed at 1000 °C, with quite regular oscillating. Jeng et al. [25] reported similar COF-scratch duration profiles when the applied ramping load was the ratio of the *in situ*-measured force tangential to nanoparticles. Chang et al. [26] also noted the abrasive wear of $Zn_{1-x}Mn_xO$ heteroepitaxial layers using a nanoscratch technique. We suggest that lower adhesion reflects the strength of the interlinks under a higher ramping load; weaker bonding of the SiGe layer resulted in the jumped lateral force as well as lower values of COF (Fig. 3).

In a previous study [15] of the effects of annealing treatment on 500-nm-thick SiGe films, we observed a cohesive failure mechanism. Herein, we subjected 200-nm-thick SiGe epilayers as samples for thermal treatment and observed cohesive strength. These SiGe epilayers were in the metastable condition, because their thicknesses were less than the critical thickness (500 nm thick) [22,23]. Therefore, during high-temperature thermal treatment, strain relaxation was more stable for a thickness of 200 nm. Notably, the friction force reflected a sliding mechanism upon varying the annealing temperature, with stronger cohesive properties of the thin films. The nanoscratch tests suggested that the hardness increased, through strain relaxation, after thermal treatment; greater susceptibility to plastic deformation was also induced through additional dislocation-propagation strain.

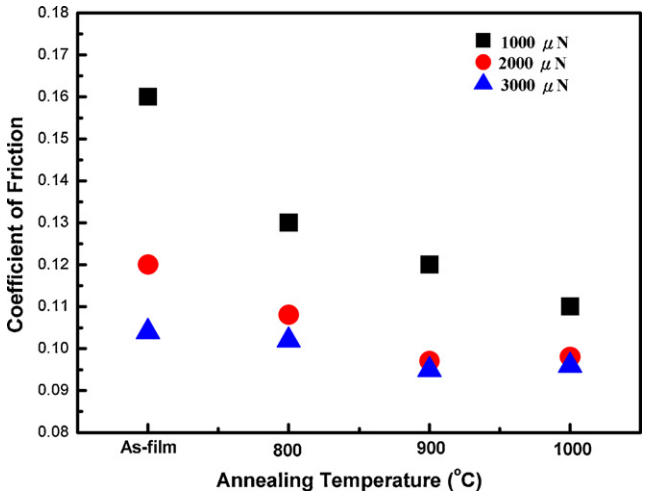

Fig. 3. Distinct critical COF respect to the as-deposited and thermal treatment of SiGe thin films.

Dislocation glide and dislocation pinning at each interlayer both play important roles in the hardening mechanisms. Noted that, the role of strain relaxation can be attributed by means of thermal treatment, hence the dislocation not only leads to hardening but also plays a critical candidate to change the cohesive failure mechanism. We suggest the metastable SiGe epilayers is easy to diffuse Si substrate each other that may induce cohesive force. The deep profile distributions of the SiGe epilayers at RT suggest that they were softer than the annealed samples. Thus, the transition from purely elastic to elastoplastic contact was revealed in the nanoscratch traces and in the depth of the pile-up. In closing, the features in the COF curves obtained from the nanoscratch system were independent of the variation of the loading conditions, indicating the real signal in the SiGe epilayer structures. Because the results from the AFM images (Fig. 1) were comparable with those from the oscillating profiles (Fig. 2), we believe that ductile-regime machining (elastoplastic deformation) of the scratch track occurred under a ramped force of 2000 μN, whereas more-plastic deformation of the scratch track occurred when the ramped force was 3000 μN. Variation of the annealing temperature led to a slight decrease in COF compared with the actual value (Fig. 3).

4. Conclusion

We have used UHV/CVD methods to prepare high-quality relaxed 200-nm-thick SiGe epilayers and employed AFM and nanoscratch tests to examine their physical properties. From a comparison of scratch events, we found deformations ranging from plastic to elastic and variations of the depth profiles under the scratch path. The friction force was applied using a sliding mechanism, revealing the cohesive properties of the SiGe epilayers. The as-deposited SiGe was weaker (higher COF) than were the annealed SiGe films in terms of their cohesive characteristics. We used nanoscratch testing to investigate variations in the tribological behavior of the SiGe epilayers. The μ profiles of the SiGe epilayers changed from oscillating relatively irregularly to oscillating rather regularly upon increasing the annealing temperature, revealing a change from weak to strong bonding, allowing us to identify the cohesive failure from the period of transition.

Acknowledgments

We thank Dr. H.C. Wen for help with this work and contributions during the initial stages of this work. This study was supported in part by the National Science Council 291 in Taiwan under contract NSC 99-2221-E-009-031-MY2. We thank 292 the National Nano Device Laboratories (contracts NDL99-C03S-293 042) for technical support.

References

[1] P. Gaworzewski, K.T. Helmrich, U. Penner, N.V. Abrosimov, J. Appl. Phys. 83 (1998) 5258.
[2] R. People, J.C. Bean, D.V. Lang, A.M. Sergent, H.L. Stormer, K.W. Wecht, Appl. Phys. Lett. 45 (1984) 1231.
[3] K. Ismail, J.O. Chu, B.S. Meyerson, Appl. Phys. Lett. 64 (1994) 3124.
[4] A. Khakifirooz, D.A. Antoniadis, Tech. Dig.—Int. Electron Devices Meet. (2006) 667–668.
[5] D.A. Antoniadis, I. Aberg, C. Ni Chleirigh, O.M. Nayfeh, A. Khakifirooz, J.L. Hoyt, IBM J. Res. Dev. 50 (2006) 363.
[6] C.W. Leitz, M.T. Currie, M.L. Lee, Z.-Y. Cheng, D.A. Antoniadis, E.A. Fitzgerald, Appl. Phys. Lett. 79 (2001) 4246.
[7] M.L. Lee, E.A. Fitzgerald, Tech. Dig.—Int. Electron Devices Meet. (2003) 429.
[8] C. Ni Chleirigh, Massachusetts Institute of Technology, Ph.D. Thesis, 2007.
[9] T. Krishnamohan, Z. Krivokapic, K. Uchida, Y. Nishi, K.C. Saraswat, Dig. Tech. Pap.—Symp. VLSI Technol. (2005) 82.
[10] C.S. Ozkan, W.D. Nix, H. Gao, Appl. Phys. Lett. 70 (1997) 2247.
[11] K. Ismail, F.K. LeGoues, K.L. Saenger, M. Arafa, J.O. Chu, P.M. Mooney, Phys. Rev. Lett. 73 (1994) 3447.
[12] Y. Atici, J. Electron. Mater. 34 (2005) 612.
[13] D.B. Aubertine, N. Ozguven, P.C. McIntyre, S. Brennan, J. Appl. Phys. 94 (2003) 1557.
[14] Y. Shiraki, A. Sakai, Surf. Sci. Rep. 59 (2005) 153.
[15] T.Y. Lin, H.C. Wen, Z.C. Chang, W.K. Hsu, C.P. Chou, C.H. Tsai, D. Lian, J. Phys. Chem. Solids 72 (2011) 789.
[16] A. Agarwal, N.B. Dahotre, L. Riester, T.S. Sudarshan, Surf. Eng. 17 (2001) 495.
[17] S. Dong, B.D. Beake, R. Parkinson, T. Bell, Surf. Eng. 19 (2003) 195.
[18] F. Haque, Surf. Eng. 19 (2003) 255.
[19] A.K. Keshri, S.R. Bakshi, Y. Chen, T. Laha, X. Li, C. Levy, A. Agarwal, Surf. Eng. 25 (2009) 270.
[20] B.D. Beake, G.A. Bell, S.R. Goodes, N.J. Pickford, J.F. Smith, Surf. Eng. 26 (2010) 37.
[21] T.-Y. Lin, C.-H. Tsai, W.-H. Yau, C.-P. Chou, Surf. Eng. 72 (2011) 789.
[22] B.C. He, C.H. Cheng, H.C. Wen, Y.S. Lai, P.F. Yang, M.H. Lin, W.F. Wu, C.P. Chou, Microelectron. Reliab. 50 (2010) 63.
[23] B.C. He, H.C. Wen, T.Y. Chiang, Z.C. Chang, D. Lian, W.F. Wu, C.P. Chou, Appl. Surf. Sci. 256 (2010) 3299.
[24] M.H. Lin, H.C. Wen, Y.R. Jeng, C.P. Chou, Nanoscale Res. Lett. 5 (2010) 1812.
[25] Y.R. Jeng, H.C. Wen, P.C. Tsai, Diamond Relat. Mater. 18 (2009) 528.
[26] Y.M. Chang, H.C. Wen, C.S. Yang, D. Lian, C.H. Tsai, J.S. Wang, W.F. Wu, C.P. Chou, Microelectron. Reliab. 50 (2010) 1111.